Available online at www.sciencedirect.com
ScienceDirect
Journal of Sound and Vibration 310 (2008) 394–408
JOURNAL OF SOUND AND VIBRATION
www.elsevier.com/locate/jsvi

Characterization of the high-frequency squeal on a laboratory brake setup

Oliviero Giannini[a,*], Francesco Massi[b]

[a]*Department of Mechanics and Aeronautics, University of Rome "la Sapienza", Via Eudossiana 18, 00184 Rome, Italy*
[b]*LaMCoS, INSA-Lyon, CNRS UMR5259, F69621, France*

Received 25 September 2006; received in revised form 20 July 2007; accepted 4 August 2007
Available online 24 October 2007

Abstract

This paper presents an experimental investigation on high-frequency brake squeal noise conducted on an appropriately designed experimental rig, called laboratory brake.

Brake squeal is one of the major issues in the design process of an automotive brake and the development of a robust procedure for a "squeal-free" design is still under investigation. The high-frequency squeal is the most frequent noise generated by automotive brakes and is characterized by a wavelength of the "squealing mode" comparable to the length of the brake pad.

The proposed "laboratory brake" is a good compromise between simple test rigs, such as the beam-on-disc, and the experimental setups that use real brakes. The beam-on-disc setup is a useful tool to understand the mechanism leading to the instability, but it does not simulate appropriately a real brake. On the other hand, real brakes are too complex for fundamental investigation and for efficient modeling.

The experimental analysis shows a strong correlation between the length of the pad, the dynamic behavior of the system, and the squealing deformed shape. Moreover, depending on the length of the pad compared with the wavelength of the disc mode, three different kind of squeal instability may occur during experiments: the sine mode squeal, the cosine mode squeal and the rotating squeal. The latter is characterized by nodal diameters rotating during a squeal cycle.

A linear reduced model, able to reproduce the dynamic behavior of the experimental setup, is used to predict the squeal occurrence. However, such linear model is not able to predict the rotating squeal characteristic that seems to be caused by nonlinear interactions due to the contact between the disc and the caliper.
© 2007 Elsevier Ltd. All rights reserved.

1. Introduction

Brake squeal refers to high-frequency sound emissions that are generated during the braking phase and characterized by a periodic or harmonic spectrum. This phenomenon is common to both drum and disc configurations and concerns both train and automotive brakes. Therefore, the geometry and the dimension of brakes can vary widely, thus leading to very different sets of squeal frequencies and associated modes.

*Corresponding author. Tel.: +39 644585556; fax: +39 6484854.
E-mail address: oliviero.giannini@uniroma1.it (O. Giannini).

0022-460X/$ - see front matter © 2007 Elsevier Ltd. All rights reserved.
doi:10.1016/j.jsv.2007.08.009

During the past years several researchers developed their study on brake squeal using simplified experimental rigs, among the others: Akay et al. [1], Algaier et al. [2], Tuchinda et al. [3], developed their researches on the beam on disc setup, and found good agreement between the squeal occurrence and the results of their models. However, it is not simple to extend such models to the study of real brakes. Therefore, an intermediate setup was designed [4–6], the laboratory brake. This setup is simple enough to permit an easy modeling, but approaches, more realistically than the beam on disc, a real automotive brake apparatus. Thus, the laboratory brake can be considered as the *''trait d'union''* between the beam-on-disc setup and a commercial brake. Moreover, this setup, used to study the low-frequency squeal, allowed for the development of a consistent model [7] that is able to predict the squeal events occurring during experiments [4].

In Refs. [8,9] a setup that represents a different improvement of the beam-on-disc is presented. This setup, called ''TriboBrake'', is particularly suited to study the correlation between squeal occurrence and the pad, the caliper and the disc dynamics, and to investigate tribological aspects of the squeal instability.

Following the idea that for high-frequency squeal there is still lack of knowledge about the physic of squeal and that a comprehensive understanding of the relation between the dynamics of the brake system and the squeal characteristic is still missing, an experimental investigation on high-frequency squeal is conducted using a modified laboratory brake. In particular this paper addresses some specific topic:

- the qualitative differences between low- and high-frequency squeal events;
- the influence of the pad dimension on the squeal characteristics;
- the modeling and the prediction of the squeal occurrences retrieving also the specific characteristics of the squeal event.

Therefore, the Laboratory Brake is modified to account for the ratio between the wavelength of the squeal deformed shape and the dimension of the zone of contact.

The paper is divided into three parts: first the experimental setup is presented along with its dynamic characterization. Then, the high-frequency squeal arising during experiments is presented and it is correlated to the dynamic behavior of the system; the third section presents the reduced model of the rig that is adopted to predict the squeal behavior of the setup.

The agreement between experimental and numerical results allows interpreting the squeal characteristics in function of the pad dimension. The phenomenon of ''traveling squeal'' is also found and analyzed both experimentally and numerically.

Since a simplified experimental rig is used, not all the results obtained can be exported as they present in this study to the squeal arising in a commercial brake apparatus; nevertheless, some important aspects can provide reliable data useful to guide the investigation conducted on real brakes that is the final aim of this work.

2. The experimental setup

Fig. 1 shows a schematic of the setup that consists of a steel disc that has a diameter of 358 mm and is 25 mm thick. The disc is held by two bearings that are attached to an aluminum frame fixed to a table. An electric motor rotates the disc. Fig. 2a shows a picture of the setup.

The HF squeal involves a deformed shape of the disc that has a wavelength comparable with the brake pad length. To simplify the study of this problem instead of a standard brake pad, two small pads ($5 \times 10\,\text{mm} = 50\,\text{mm}^2$) are used, assuming the distance d between them as the characteristic length of the pad (Fig. 2b).

In the laboratory brake, the caliper consists of a steel beam[1] that holds the two brake pads that are obtained by machining a commercial brake pad.

A thin aluminum plate holds the beam in the friction force direction (the direction of the relative velocity) while applying a negligible force in the normal direction (the direction of the normal load). A support connects the aluminum plate to the table.

[1]Same results were obtained when two beams were holding the disc on both faces, as in Ref. [4]. The authors preferred to use for this study only one beam in order to have a side of the disc easily attainable for the use of a vibrometer laser scanner to allow a measure of the vibrations of the rotor in the contact sector.

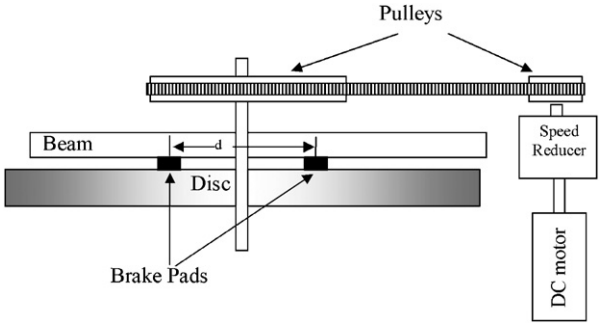

Fig. 1. Schematic of the laboratory brake setup.

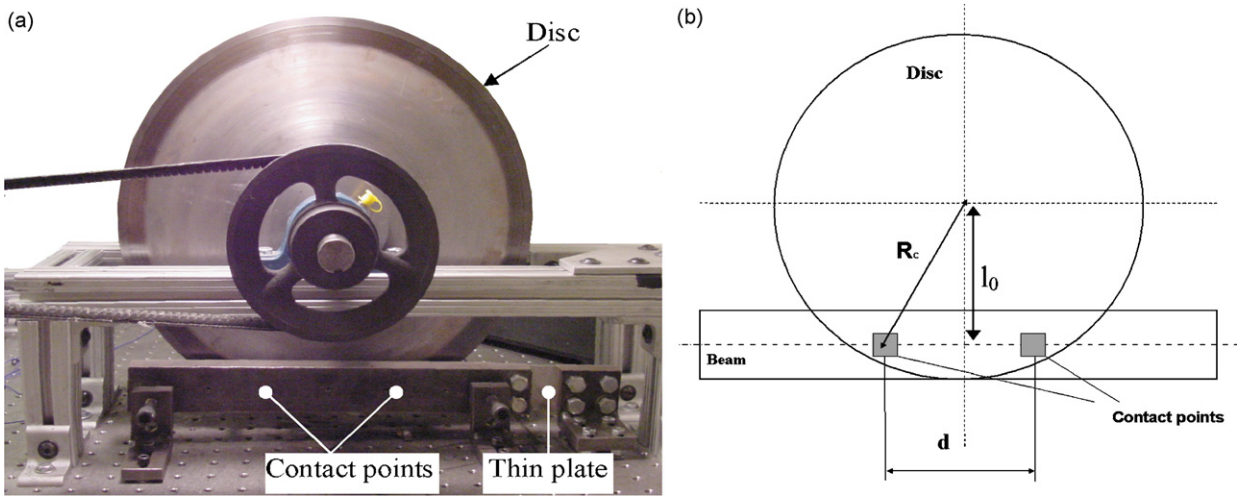

Fig. 2. The laboratory brake setup (a) picture of the setup; (b) contact points arrangement.

The two brake pads are located along the axes of the beam and the distance d can be changed from test to test. The distance between the rotor center and the beam axis is $l_0 = 162\,\text{mm}$.

The laser scanner vibrometer is used to measure the operational deflection shapes of the disc and the beam during hammer tests as well as the squeal deformed shape during squeal events.

The use of two small pads, instead of a commercial brake pad is the key simplification introduced in this setup. In fact, it is possible in this way to maintain a low coupling between the disc and the beam, so that the dynamic behavior of the system can be easily interpreted in terms of the dynamic behavior of its components, while studying the effect of the length of the contact on the squeal behavior.

Unfortunately this solution does not permit to consider the effect of the torsional modes and of high-order bending modes of the pad.

2.1. Analysis of the dynamic behavior of the setup

To provide the reference behavior for the experimental setup, an experimental modal analysis is performed on the laboratory brake components that are the beam and the disc when they are not in contact to one another. In the following this condition is referred as "uncoupled condition".

Disc modes are characterized by nodal circumferences and nodal diameters: the disc modes (n,m) is characterized by n nodal circumferences and m nodal diameters. Since the disc is axial symmetric the modes of the disc are generally double modes.

The test results for the uncoupled case provide a reference behavior for the laboratory brake as well as the data necessary to build the reduced model of the setup (see Section 3.1). Table 1 lists, the natural frequency of the laboratory brake components.

A further dynamic analysis is conduced on the assembled brake system.

As a result of the contact with the pads, the disc loses its axial symmetry and the modes of the disc with double eigenfrequencies split;

The following notation is used to label the split system modes:

- mode $(n,m-)$: a nodal diameter is coincident with the center of the contact area (i.e. the middle point between the two pads). These modes are also called *sine modes*.
- mode $(n,m+)$: an antinode is coincident with the center of the contact area. These modes are also called *cosine modes*.

Several hammer tests were performed to retrieve the dynamic behavior of the system as the distance between the pads increases.

The natural frequencies of the coupled system mainly depend on the normal load, and the distance between the pads. For a given normal load, it is possible to observe (Fig. 3) that, as the distance between the pads changes, the natural frequency of the modes of the rotor oscillates. Moreover, the frequency separation between two modes derived from the split of a double mode of the free rotor, first decrease (e.g. for the (0,5) mode of the rotor for $0\,\text{mm} < d < 51\,\text{mm}$), to increase, again, up to maximum value ($d = 106\,\text{mm}$ for the (0,5) mode), to decrease again for higher value of d. Table 1 presents the average value of the natural frequencies of the coupled rotor measured during the tests for several distances between the pads.

Because the likelihood of a mode to squeal is dependent on the comparison between its wavelength and the dimension of the contact zone, to generalize this analysis and to correlate the observations taken from different modes, the results are presented in terms of split between the frequencies as a function of the ratio $r = d_\alpha/\lambda$ where $d_\alpha = 2\ tg^{-1}(d/2l_0)$, d is the distance between the two brake pads and λ is the wavelength of the considered mode measured along the chord.

Table 2 shows the value of the distance between the pads and the corresponding value of the ratio r for the considered modes of the rotor.

Fig. 4 shows the operative deformed shapes of the modes (0,5−) and (0,5+) measured with the laser scanner during these tests for $r = 0$, $r = 0.25$, and $r = 0.5$ respectively.

Table 1
Natural frequency of the laboratory brake

Mode	Natural frequency (Hz); uncoupled disc and beam	Average frequency (Hz); coupled system	Squeal frequency
(0,3)	1820	1912	1910–1920
2nd beam	2340	2407	
(1,1)	2630	2745	
(0,4)	3110	3176	3140–3180
3rd beam	4180	4237	
(0,5)	4660	4695	4670–4700
(1,2)	5100	5177	
(0,6)	6430	6446	6440–6460
4th beam	6840	7004	
(1,3)	7180	7329	
(0,7)	8380	8395	8390–8400
(1,4)	N.A.	9569	
(0,8)	N.A.	10506	10,500
(1,5)	N.A.	12130	
(0,9)	N.A.	12840	12,850

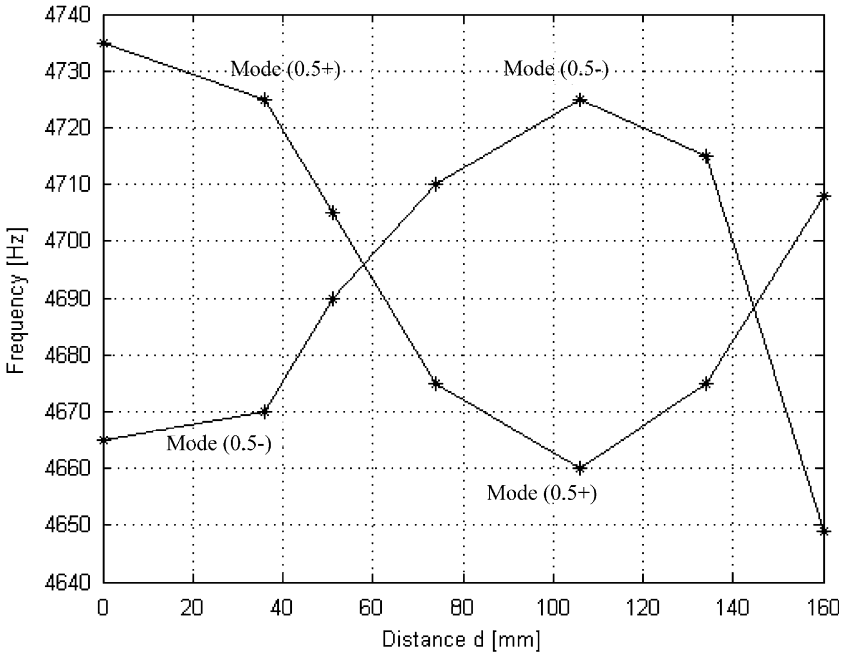

Fig. 3. Natural frequencies of the mode (0,5) pair as the distance between the two pads changes.

Table 2
Distance between the pads and corresponding value of the ratio r

d (mm)	r for (0,4)	r for (0,5)	r for (0,6)	r for (0,7)	r for (0,8)	r for (0,9)
0	0	0	0	0	0	0
36	0.14	0.18	0.21	0.25	0.28	0.32
42	0.16	0.21	0.25	0.29	0.33	0.37
51	0.20	0.25	0.30	0.35	0.40	0.45
74	0.29	0.36	0.43	0.50	0.57	0.64
106	0.40	0.50	0.60	0.70	0.81	0.91
134	0.50	0.62	0.75	0.87	1.00	1.12

Fig. 4 shows that for $r = 0$ the two contact points fall on the nodal diameter of the (0,5−) mode and on an antinodal diameter of the (0,5+), causing the split to be maximum. In fact, in this case the latter mode is highly influenced by the contact with the pads, while the former is not, and it remains at the same frequency of the (0,5) mode, measured in uncoupled conditions. Vice-versa, the opposite occurs for $r = 0.5$.

If $r = 0.25$, the amplitude of the disc displacement at the contact points is the same for both the modes; the two modes are equally influenced by the contact and their frequency returns to be equal. In these conditions the modes of the disc become double modes again.[2]

By representing these results as a function of r, it is possible to compare the dependency of the split of all the modes of the rotor on the length of the pad. In fact, the behavior described above is the same for all the modes of the disc. Fig. 5 shows the split of all disc modes in the studied frequency range as a function of the ratio r. The split is assumed to be positive if the mode $(n,m+)$ is at a lower frequency with respect to the corresponding $(n,m-)$ mode.

[2]In this paper two modes are considered a double mode when the separation in frequency is lower than the available frequency resolution available in the experimentation that is usually 0.5Hz.

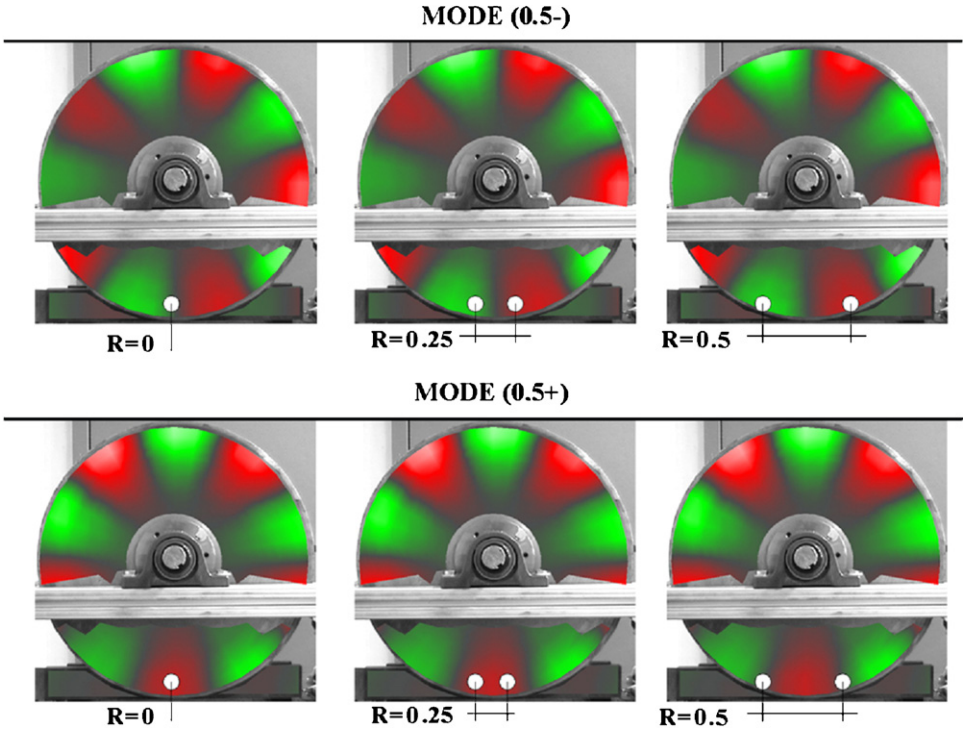

Fig. 4. Operative deformed shape of the (0,5+) and (0,5−) modes of the disc for $r = 0$, $r = 0.5$, and $r = 0.5$.

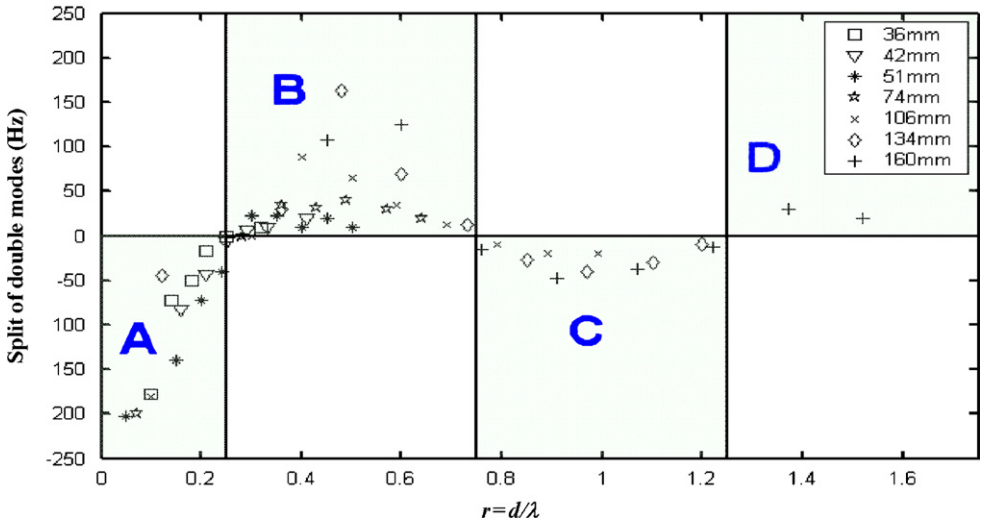

Fig. 5. Split of the disc modes for different values of the ration r.

The plot is divided into four different regions named from A to D: in zone A and C, i.e. for $0 < r < 0.25$ and for $0.75 < r < 1.25$ the $(n,m+)$ modes are at a higher frequency with respect to the corresponding $(n,m-)$ mode, so that the split is negative. For $r = 0.25$, $r = 0.75$ and $r = 1.25$ the measured split is almost zero.

Particular attention is devoted to the characterization of the pad dynamics; Fig. 6 presents the power spectral density measurements for the in-plane and out-of-plane vibrations of one of the pads. The in-plane vibrations are measured with an accelerometer put on the pad with its axis in the same direction of the relative velocity; the out-o-plane vibrations are measured on the beam in a point coincident with the pad location.

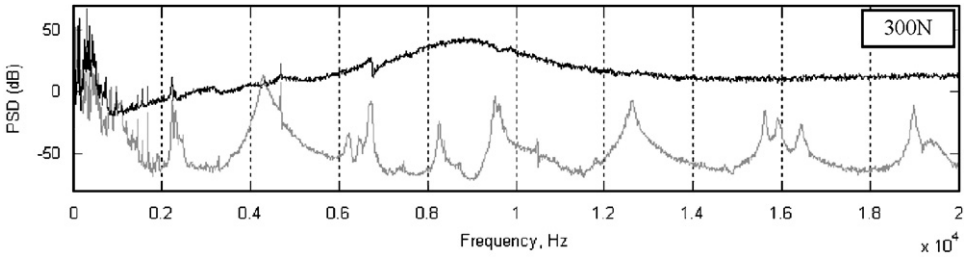

Fig. 6. Power spectral density of the pad acceleration: in-plane (black) and out-of-plane (gray).

These measurements are made after 100 cycles following insertion of new pads, the disc rotation speed was kept at 10 rev/min for normal loads of 300 N.

The out-of-plane response (gray line) in Fig. 6 contains all the system frequencies. The in-plane response of the pad (dark line) also exhibits some of the same frequencies but less prominently than the out-of-plane response. In addition, however, the in-plane response contains a highly damped spectral peak at 9 kHz that is a shear natural frequency of the pad.

2.2. Experimental analysis of the squeal behavior of the setup

The measurements performed to characterize the squeal behavior of the setup are aimed at understanding, for a given configuration of the system, which modes may become unstable. In order to establish a reliable relation between possible instabilities and length of the pad, several tests are performed. The tests procedure can be summarized as follows:

1. the distance between the two pads is set and the setup is assembled;
2. the disc starts rotating and the normal load is adjusted until squeal develops;
3. a vibrometer laser scan of the disc and the beam surface is performed in order to measure the squealing deformed shape. An accelerometer located on the beam in the meddle point between the pads provides the reference signal;
4. after the acquisition, the normal load is changed to look for a different squeal frequency.

These steps are performed for different distances between the pads (Table 1).

The squeal sound observed usually has a periodic spectrum with the magnitude of the fundamental frequency higher than its sub-harmonics from 20 to 80 dB, depending on the test conditions. The fundamental frequency is always close to a natural frequency of the coupled system. As a result, the vibration response of the system is nearly identical to the corresponding operative deformed shape, which can be measured with the laser scanner during a hammer test.

The squeal events are characterized by a fast exponential growth of the vibration of the system, during this phase the signal is almost an exponentially increasing sinusoid. Then the amplitude stabilizes into a limit cycle, super harmonics appear and the nonlinear aspects of the contact (mainly local detachment between disc and pads) determine the amplitude of the cycle [9].

Depending on the distance between the contact points (length of the pad) with respect to the wavelength of the disc mode three different kind of squeal instability were identified during experiment:

- the sine mode, characterized by fixed nodal diameters and a $(n,m-)$ mode squealing;
- the cosine mode, characterized by fixed nodal diameters and a $(n,m+)$ mode squealing;
- the rotating squeal, characterized by nodal diameters rotating during the squeal vibration.

Table 3 lists the squeal occurring during these tests. The table presents the squealing disc modes, the distance between the two pads and, the ratio r for each mode involved in the squeal. For each distance between the pads and each mode of the system involved in squeal, the corresponding value of the ratio r is displayed in the appropriate cell.

Table 3
Squeal occurrences during experiments for different distance between the pads

Distance / Mode	D= 0	D= 36	D= 42	D= 51	D = 74	D= 106	D= 134	D = 160	D=168
(0,4)					r=0.29				
(0,4+)	r=0			r=0.20					
(0,5)		A		**r=0.25**	r=0.36	r=0.50			
(0,5+)	r=0								
(0,6)			Rotating r=0.25	r=0.30	r=0.43	r=0.60	Rotating r=0.75	C	
(0,6+)	r=0								
(0,7)		Rotating r=0.25	r=0.29	B	r=0.50				
(0,7+)	r=0					**r=0.7**	r=0.87		r=1.11
(0,8)		r=0.28	r=0.33	r=0.40	r=0.57	Rotating r=0.78		Rotating r=1.27	r=1.28
(0,8+)	r=0						r=1		
(0,9)			r=0.37	r=0.45				r=1.52	r=1.43
(0,9+)	r=0					r=0.91	r=1.12		D

For example, for a distance $d = 106$ mm, five squeal conditions are found: 2 involving sine modes, the (0,5−) and the mode (0,6−); a rotating squeal involving the (0,8) mode; two cosine modes (0,7+) and the (0,9+).

Table 3 is divided into four regions, reflecting the division made in Fig. 5. Squeals in zones A and C are characterized by the $(n,m+)$ modes squealing, while in regions B and D the $(n,m-)$ modes become unstable. We can summarize this by stating that, between the two split modes, derived from a double mode of the disc in uncoupled conditions, it is generally the mode at higher frequency that is involved in the squeal instability.

This can be explained by considering that the larger is the modal displacement of the rotor at the contact points, the larger is the coupling introduced by the contact. Large coupling has two effects [8]: first, it increases the coupled natural frequency with respect to the uncoupled one (the peak is the one at higher frequency); second, it increases the energy transfer from the tangential continuous rotation of the disc to the out-of-plane vibrations of the system (higher propensity to squeal).

During the experiments only two squeal cases, represented by bold characters in the table, do not satisfy this statement:

- the squeal of the mode (0,5) for $d = 51$ and $r = 0.24$;
- the squeal of the mode (0,7+) for $d = 106$ and $r = 0.69$.

Two different explanations may justify this discrepancy:

(1) these two cases have a value of r that is close to the boundary between the regions so that, in these conditions, the coupling may occur for both $(n,m+)$ and $(n,m-)$ modes.
(2) there is an inevitable error in measuring the distance d between the two pads considered as a contact point instead of taking into account the real contact surface.

Particulary interesting is the rotating squeal that may develop at the boundary between the zones highlighted in Table 3. In fact, when the two split modes have again the same frequency, i.e. for $r = 0.25$, $r = 0.75$, and $r = 1.25$, both modes squeal together causing the squeal deformed shape not to be stationary anymore, but rather, the nodal lines rotate during a squeal period as found in commercial brakes by Fieldhouse et al. [10–12]. In this case the two stationary waves related to the $(n,m+)$ and $(n,m-)$, that have "per definition" 90° phase difference in space, may combine to produce the traveling wave observed

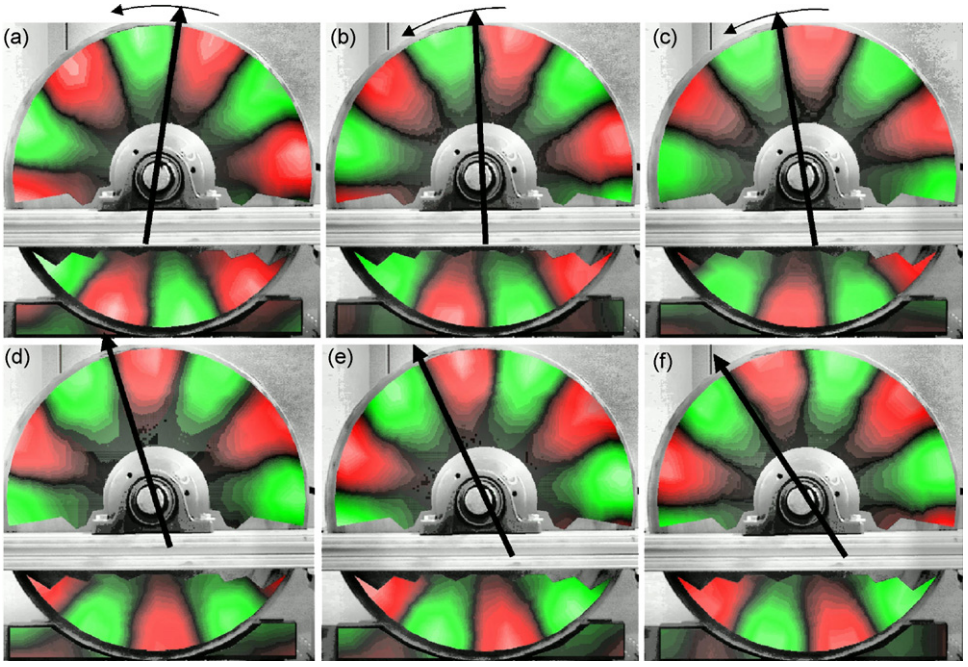

Fig. 7. (0,6) Mode rotating squeal at 6400 Hz, from *a* to *f* six frames of the rotating squealing shape.

experimentally. It is worthwhile to note that in order to have a pure traveling wave, the two stationary waves must have same amplitude and a 90° phase difference in time.

During the experiments, the rotating squeal events involve:

- the mode (0,6) for $r = 0.25$
- the mode (0,7) for $r = 0.25$
- the mode (0,6) for $r = 0.75$
- the mode (0,8) for $r = 0.78$
- the mode (0,8) for $r = 1.27$.

Fig. 7a–e shows 6 frame of the (0,6) rotating squeal at 6400 Hz.

3. Reduced order model of the laboratory brake

In Ref. [7] the authors presented a reduced order model able to predict the low-frequency squeal occurring in the laboratory brake. This model is here modified to account for two contact points.

The model starts from data derived from the experimental modal analysis of the laboratory brake components: the beam and the disc. Other two degrees of freedom are added to account for the dynamics of the pad. Since each pad has a small area in contact with the disc, it is assumed as a point contact. Each pad is modeled by a one rotational degree of freedom (Fig. 8) defined by an inertia J_p and a stiffness k_p. If there is not contact between disc and pad, the system mass and stiffness matrices are:

$$\mathbf{K}_0 = \begin{bmatrix} [\mathbf{\Lambda}_{d1}] & 0 & 0 & 0 & 0 & 0 \\ 0 & [\mathbf{\Lambda}_{d2}] & 0 & 0 & 0 & 0 \\ 0 & 0 & [\mathbf{\Lambda}_b] & 0 & 0 & 0 \\ 0 & 0 & 0 & [\mathbf{\Lambda}_b] & 0 & 0 \\ 0 & 0 & 0 & 0 & k_p & 0 \\ 0 & 0 & 0 & 0 & 0 & k_p \end{bmatrix} \quad \mathbf{M}_0 = \begin{bmatrix} [\mathbf{I}] & 0 & 0 & 0 & 0 & 0 \\ 0 & [\mathbf{I}] & 0 & 0 & 0 & 0 \\ 0 & 0 & [\mathbf{I}] & 0 & 0 & 0 \\ 0 & 0 & 0 & [\mathbf{I}] & 0 & 0 \\ 0 & 0 & 0 & 0 & J_p & 0 \\ 0 & 0 & 0 & 0 & 0 & J_p \end{bmatrix}. \tag{1}$$

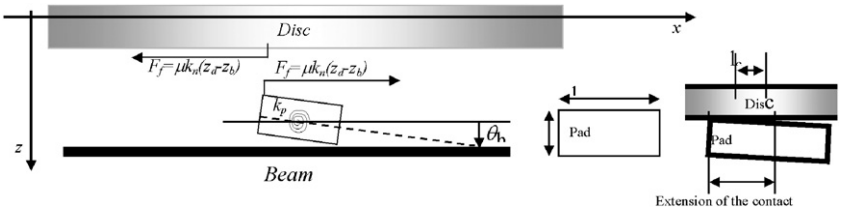

Fig. 8. Model of the pad as a rotational one degree of freedom system.

In the out-of-plane direction the pad is modeled by a lumped stiffness k_n. When there is contact between disc and pad the modes of the disc and the beam are coupled together through k_n.

The elastic force acting on the disc, due to relative displacement between disc and beam, can be written as

$$F_e = k_n(z_d - z_b)\delta(x - x_0)\delta(y - y_0) \tag{2}$$

and the modal force F_i^m acting on the ith mode of the disc is

$$F_i^m = \iint_d \Phi_i F_e \,\mathrm{d}x\,\mathrm{d}y = \iint_d \Phi_i k_n(z_d - z_b)\delta(x - x_0)\delta(y - y_0)\,\mathrm{d}x\,\mathrm{d}y = \Phi_i^P k_n(z_d - z_b). \tag{3}$$

Φ_i is the ith mode of the uncoupled disc; z_d and z_b are the disc and beam out-of-plane physical displacements and δ is the Dirac function. Φ_i^P is the mode evaluated at the contact point $P(x_0,y_0)$.

The displacements of the disc and the beam can be expressed by a linear combination of the modal displacements so that

$$F_i^m = \Phi_i^P k_n\left(\sum_{i=1}^{Nb} \Psi_i^P p_i - \sum_{i=1}^{Nd1} \Phi_i^P q_i\right), \tag{4}$$

where Ψ_i^P is the ith mode of the beam, p_i and q_i are the modal displacements of the disc and the beam, respectively, and N_d and N_b are the number of modes of the disc and the beam, included in the model. These elements are not diagonal anymore and form the coupling system stiffness matrix $\mathbf{K}$:

$$\begin{aligned} K_{i,j} &= \Phi_i^P k_n \Phi_j^P \quad \forall \quad 1<i<N_d, 1<j<N_d, \\ K_{i,j+N_{d1}+N_{d2}} &= -\Phi_i^P k_n \Psi_j^P \quad \forall \quad 1<i<N_d, 1<j<N_b. \end{aligned} \tag{5}$$

In the same way all the others coupling terms of the matrix due to the elastic interaction in the out-of-plane direction are added.

Under the assumption that the maximum in-plane velocity of the pad is always smaller than the velocity of the disc at the contact points, so that stick-slip motion does not occur [4], and assuming a friction coefficient that is constant with the velocity, it is possible to write the moment M_f of the friction force on the pad as

$$M_f = F_f h/2 = \mu F_N h/2 = \mu k_n(z_d - z_b\,\cos(\alpha))h/2 \tag{6}$$

that can be also expressed in terms of the modal coordinates as follows:

$$M_f = \mu k_n\left(\sum_{i=1}^{Nd1} \Phi_i^P q_i - \sum_{i=1}^{Nb} \Psi_i^P\,\cos(\alpha)p_i\right)h/2. \tag{7}$$

In this way, the terms in the system stiffness matrix are:

$$\begin{aligned} K'_{i,j} &= -\mu k_n \Phi_j^P h/2 \quad \forall \quad i = N_s + 1, \;\; 1<j<N_d, \\ K'_{i,j+N_{d1}+N_{d2}} &= \mu k_n \Psi_j^P h\,\cos(\alpha)/2 \quad \forall \quad i = N_s + 1, \;\; 1<j<N_b. \end{aligned} \tag{8}$$

The feed-back force, i.e. the force that the rotation of the pad applies to the disc and the beam, can be expressed as

$$K'_{i,j} = k_n \Phi_i^P l_c \quad \forall \quad 1<i<N_d, \ j = N_s + 1,$$
$$K'_{i+N_{d1}+N_{d2},j} = -k_n \Psi_i^P \cos(\alpha) l_c \quad \forall \quad 1<i<N_b, \ j = N_s + 1. \tag{9}$$

The terms in Eq. (9) are symmetric. When the disc is deformed, the stiffness k_n causes a torque on the pad:

$$K'_{i,j} = k_n \Phi_i^P l_c \quad \forall \quad i = N_s + 1, \ 1<j<N_d,$$
$$K'_{i,j+N_{d1}+N_{d2}} = -k_n \Psi_i^P \cos(\alpha) l_c \quad \forall \quad i = N_s + 1, \ 1<j<N_b. \tag{10}$$

The above assumption on the friction force leads to a simple linear model of the coupled system, that has a stiffness matrix that is not symmetric.

3.1. Discussion of the model

The proposed model accounts for the out-of-plane dynamics of the laboratory brake through the uncoupled bending modes of the disc and the beam that can be accurately measured. Since these measurements are performed in uncoupled condition, i.e. when the disc and the beam are not in contact, the modes are not affected by any uncertainty or nonlinearity related to the pads. The in-plane dynamics of the disc is not included in the model because it was verified that the first rotational mode of the disc is around 800 Hz and falls below the frequency range of interest,[3] while the other in-plane modes are above 10 kHz. Moreover, during the experiments, squeal occurs only at frequencies corresponding to bending modes of the disc or the beam. At these frequencies the in-plane vibrations of the disc are negligible with respect to the out-of-plane ones.

The small brake pads are modeled in the out-of-plane direction by a stiffness connection between the disc and the beam; such simplification is acceptable for the aim of this study because the wavelengths related to the squealing bending modes are much larger than the length of each pad, so that the pressure distribution along the contact surface, may be represented by its average.

The dynamic characteristics of the pads in the model are its moment of inertia J, the out-of-plane stiffness k_n, and its rotational eigenfrequency. The value of k_n can be evaluated experimentally [7], the effective moment of inertia J can be obtained through a FEM of the pad, while the rotational eigenfrequency of the pad is considered highly variable and need further explanations.

In the laboratory brake, the experimental results in Refs. [4,7] showed that the 1st in-plane natural frequency of each pad can vary largely. This is mainly due to the fact that given its small size its dynamic is largely affected by the contact conditions (i.e. variations of the contact conditions are due to normal load variations and effective extent of the contact between each pad and the rotor); moreover, the wear of the pad can have a consistent influence on its dynamics.

Therefore, it is convenient to perform the complex eigenvalue analysis in function of the eigenfrequency of the pad.

A last consideration concerns the contact law: in the literature many authors use a constant friction coefficient and the assumption of no stick-slip behavior [3,13–16]. The transient dynamic numerical analysis performed in Ref. [9] showed the absence of the stick-slip during squeal simulations. The experimental results in Ref. [4] show that, during the squeal limit cycle, the maximum in-plane velocity is between 30% and 50% of the average rotational velocity of the disc. This difference assures that measurement errors or variation in the rotational velocity would not cause any change in the direction of the relative velocity. Moreover, the onset of instability occurs when the in-plane vibration of the pad is two orders of magnitude lower than the amplitude of the squeal limit cycle, implying that the onset of instability can develop in non-stick-slip conditions.

Final consideration concerns the linearity of the model that may only be used to detect possible unstable solutions and the first few instant of the squeal vibration, while squeal is characterized by an exponential growth. It is not possible to derive from a linear model the amplitude of the limit cycle that is due to nonlinear effect related to the contact [9]. Therefore, the aim of the model is only to predict the unstable modes as the distance between the pad changes and to verify the dependency between the onset of the instabilities and the dynamics of the system.

[3]Squeal events below 2 kHz did not occur during the experimental investigation.

3.2. Complex eigenvalue analysis

In order to study the squeal tendency of the setup, a stability analysis is performed on the model, and the unstable eigenvalues are equated to a possible "squealing mode".

To verify the proposed model, a comparison between the dynamic behavior of the setup and the dynamics of the model is performed. Fig. 9 presents a comparison between the eigenvalues of the model corresponding to the (0,5) mode of the disc, and the experimental results obtained for the same mode as the distance between the two pads ranges between *0* mm and 134 mm. The results show a good agreement, assuring that the parameters chosen to model the pads are consistent with the experiments.

The complex eigenvalue analysis is performed, for a given distance between the two pads, as the eigenfrequency[4] of the pads changes. In the following, as eigenfrequency of the pad is intended the quantity $f_p = \sqrt{k_p/J_p}/2\pi$, that is the eigenfrequency of the pad in uncoupled conditions. As noticed in the previous section, it is possible to shift this natural frequency during the experiments, by adjusting the configuration of the setup, from 800 Hz to 12 kHz. However, the model account for modes of the disc and the beam only up to 8 KHz, because of the limited bandwidth available during the modal analysis performed on the setup. Moreover, no squeal events where found below 3000 Hz: therefore, the reported stability analysis of the model is limited between 2.5 and 9 kHz.

Fig. 10 shows the result of the complex eigenvalues analysis performed for a fixed distance $d = 0$; the plot shows on the x-axis the eigenfrequency of the pads while, on the y-axis, the frequencies of the eigenvalues are displayed. For each value of the eigenfrequency of the pads, the eigenvalues of the model are extracted and are plotted as gray dots. If the real part of an eigenvalue is positive, this eigenvalue is plotted as a black dot.

Therefore, Fig. 10 presents a stability map of the model, highlighting by black lines the possible instabilities. The instabilities may occur when the eigenfrequency of the pads in coupled conditions, that it is the diagonal gray line, falls close to certain mode of the disc or the beam, i.e the horizontal lines. By comparing Fig. 11 with Table 1 it is possible to see a good agreement between noise frequency measured during experiments and predicted unstable eigenvalues. Moreover, comparing numerical results with Table 3 that reports the unstable modes obtained during experiments, it is possible to observe a good agreement between the two.[5]

For each unstable disc mode found, an analysis on the influence of the distance between the pads is performed. The eigenfrequency of the pads are set in order to have the maximum real part of the unstable eigenvalue for $d = 0$, and several stability analyses are performed as the angular distance between the pads ranges between 0 and 134 mm. Fig. 11a, shows these results for the (0,4) mode of the disc, Fig. 11b for the (0,5) mode, Fig. 11c for the (0,6) mode, and Fig. 11d for the (0,7) mode.

All the plots in Fig. 11 show the same qualitative behavior: for a small distance between the pads compared with the mode wavelength, i.e. when $r < 0.25$, the $(n,m+)$ mode is at higher frequency with respect to the corresponding $(n,m-)$ mode and it is unstable. While r approaches the critical value $r = 0.25$, both the eigenvalues show possible instability. If $0.25 < r < 0.75$, the $(m,n-)$ modes are at higher frequency and they are likely unstable. Thus, as highlighted by the experiments (see Table 3), the instability involves always the split mode at higher frequency. Moreover, the experimental occurrence of rotating squeal can be related to the simultaneous instability of both $(n,m+)$ and $(n,m-)$ modes, that occurs around $r = 0.25 + 0.5i$, $i = 0,1,2\ldots n$.

4. Conclusion

The proposed experimental setup and the measurements presented in this paper correlate the high frequency squeal behavior to the modal properties of the laboratory brake setup.

The setup is able to reproduce easily and, thus, study many squeal conditions; particularly interesting is the possibility of studying the rotating squeal correlating its occurrence with specific values of the parameter r which results to be the key to organize the different high-frequency squeal behaviors.

[4]For the sake of simplicity the two pads are assumed to have the same eigenfrequency. The analysis of the complex eigenvalues, performed by considering the two eigenfrequencies of the pads independent, did not added any qualitative change in the results.

[5]The instability at 4300 Hz, involving a bending mode of the beam is obtained experimentally but it is not discussed here because it is not related to a disc mode squealing.

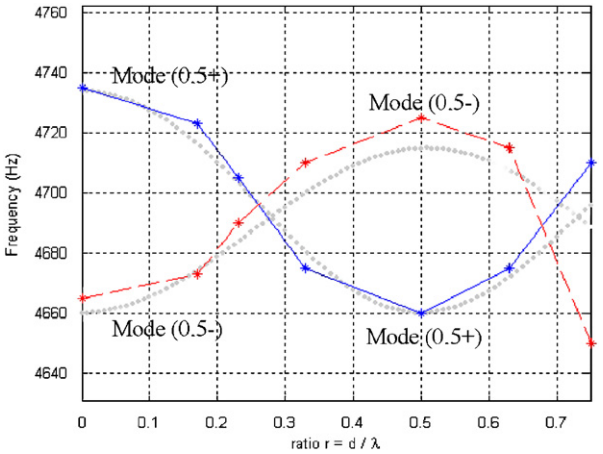

Fig. 9. Comparison between the eigenfrequencies of the (0,5+) and (0,5−) modes of the disc obtained from the experiments (dashed and continuous line) and from the model (dots) when the distance between the pads changes.

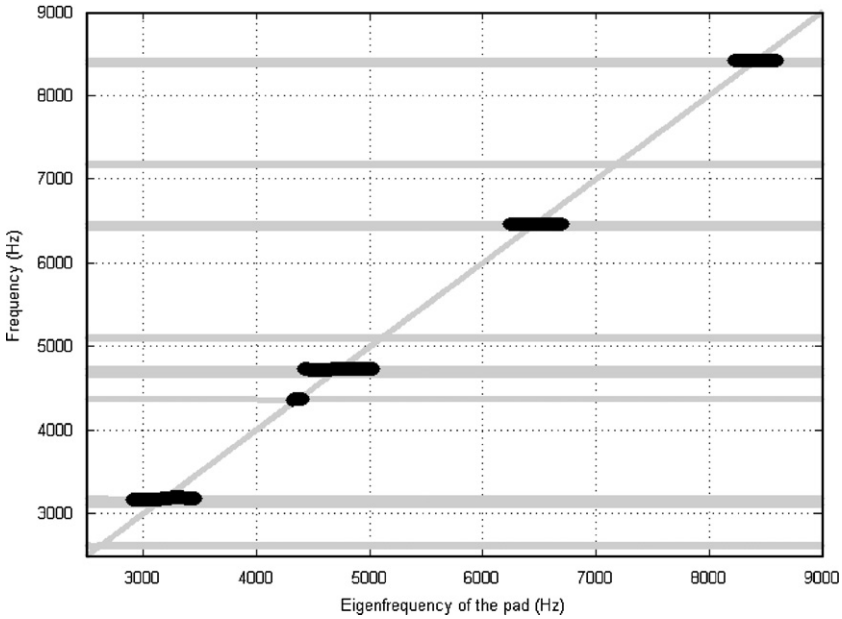

Fig. 10. Complex eigenvalue analysis performed for a distance between the pads $d = 0$.

Moreover, the results allow for a more consistent classification between low- and high-frequency squeal, based on the value of the ratio r: low-frequency squeal occurs for $r < 0.25$, while, for $r \geqslant 0.25$, rotating squeals, that are characteristic of the high-frequency squeal, can occur as well as squeals involving the $(n,m-)$ modes of the disc.

The general rule is that the squeal involving a disc mode involves the one at higher frequency between the two modes derived from the split of the double mode of the disc in "free conditions".

The presented results extend the conclusions found for the low-frequency squeal in Refs. [4,7,8] where the authors found that low-frequency squeal develops at a frequency corresponding to a natural frequency of the coupled system and involves an $(n,m+)$ mode of the disc. In fact, for the low-frequency squeal the $(n,m+)$ modes results to be always at higher frequency with respect to the corresponding $(n,m-)$ modes.

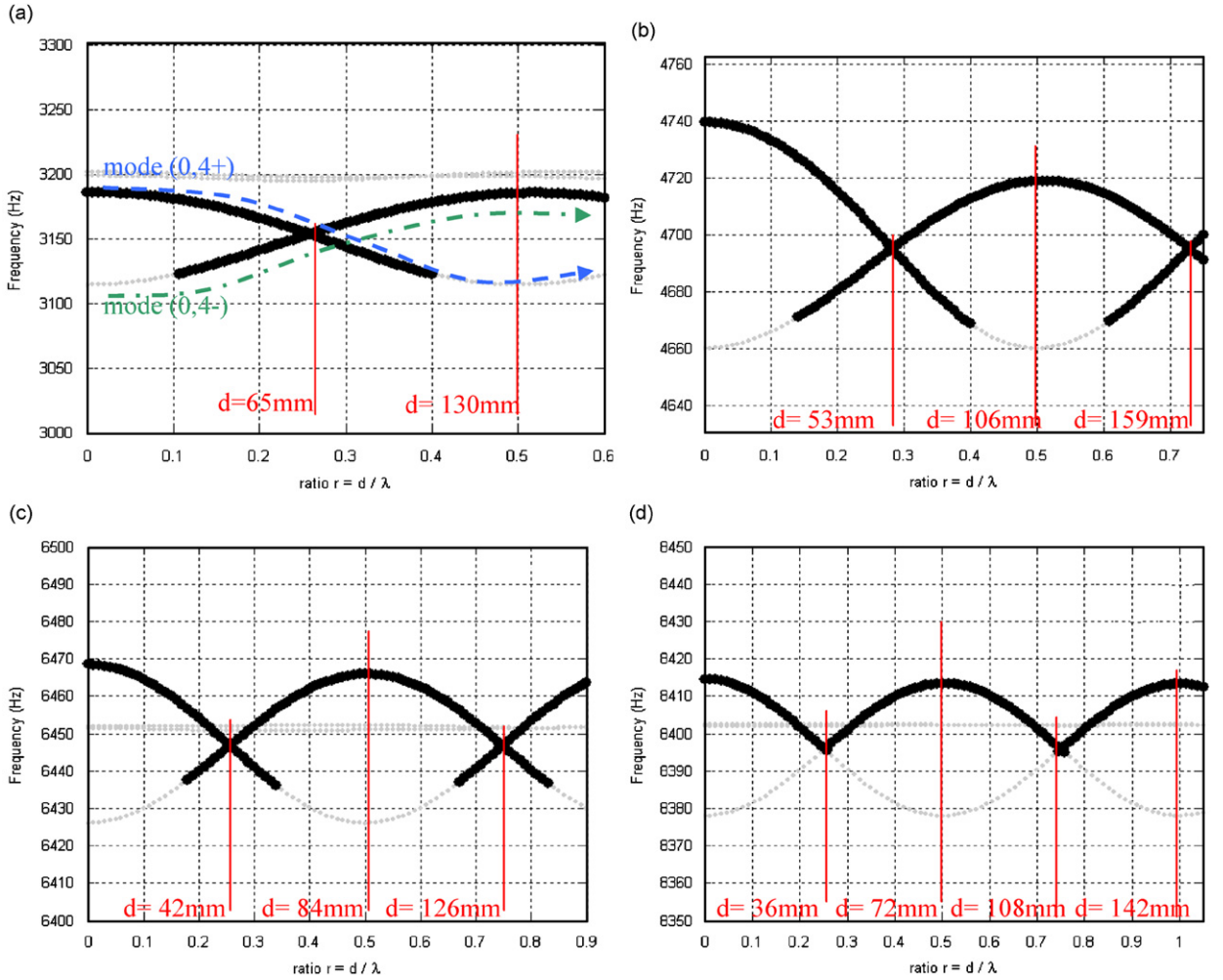

Fig. 11. Stability analysis performed as the angular distance between the pads ranges from 0° to 50°. (a) mode (0,4); (b) mode (0,5); (c) mode (0,6); (d) mode (0,7).

The proposed reduced linear model allows for an easy stability analysis that reflects the squeal instabilities found during experiments. This corroborates the idea that the squeal is a dynamic instability caused by the coupling between two modes of the brake. In the laboratory brake the squeal involves always a mode of the pad coupled with a mode of either the disc or the beam.

Occurrences of rotating squeal are strongly correlated to the value of the ratio r. To generalize this finding about rotating squeal to commercial brake, it is possible to state that a rotating squeal occurs for special contact and geometrical conditions that causes two split modes of the disc to have again very close natural frequency.

Finally the rotating squeal may be predicted as possible squeal condition based on the results of a reduced linear model. However, the possibility of modeling the actual traveling wave, needs a more sophisticated nonlinear model, including nonlinear aspects of the contact between disc and pad.

Acknowledgement

The authors would like to acknowledge the support, both personal and economical provided in these years of research on brake squeal, to Professor A. Akay and Professor A. Sestieri.

Special thank goes to Mr. Xu, who helped us during all the experimental work carried out in the years at Carnegie Mellon University.

References

[1] A. Akay, J. Wickert, Z. Xu, Investigating criteria for the onset of mode lock-in, Technical Report, Carnegie Mellon University, 1998.
[2] R. Allgaier, L. Gaul, W. Keiper, K. Willner, N.P. Hoffman, A study on brake squeal using a beam-on-disc model, *Proceedings of IMAC XX* Paper No. 363, 2002.
[3] A. Tuchinda, N.P. Hoffmann, D.J. Ewins, W. Keiper, Effect of pin finite width on instability of pin-on-disc systems, *Proceedings of the International Modal Analysis Conference—IMAC*, Vol. 1, 2002, pp. 552–557.
[4] O. Giannini, A. Akay, F. Massi, Experimental analysis of brake squeal noise on a laboratory brake set-up, *Journal of Sound and Vibration* 292 (2006) 1–20.
[5] O. Giannini, A. Akay, Z. Xu, A laboratory brake for the study of automotive brake noise, *Proceedings of IMAC XX* paper No. 373, 2002.
[6] O. Giannini, F. Massi, An experimental study on the brake squeal noise, *Proceedings of ISMA* 2004, pp. 3411–3426.
[7] O. Giannini, A. Sestieri, Predictive model of squeal noise occurring on a laboratory brake, *Journal of Sound and Vibration* 296 (2006) 583–601.
[8] F. Massi, O. Giannini, L. Baillet, Brake squeal as dynamic instability: an experimental investigation, *Journal of the Acoustical Society of America* 120 (3) (2006) 1388–1399.
[9] F. Massi, L. Baillet, O. Giannini, A. Sestieri, Brake squeal: linear and non-linear numerical approaches, *Mechanical Systems and Signal Processing* 21 (6) (2007) 2374–2393.
[10] J.D. Fieldhouse, P. Newcomb, The application of holographic interferometry to the study of disc brake noise, Technical Report 930805, SAE, Warrendale, PA, 1993.
[11] J.D. Fieldhouse, T.P. Newcomb, Double pulsed holography used to investigate noisy brakes, *Optics and Lasers in Engineering* 25 (6) (1996) 455–494.
[12] J.D. Fieldhouse, A proposal to predict the noise frequency of a disc brake based on the friction pair interface geometry, 17th Annual SAE Brake Colloquium and Engineering Display, Florida, October 10–13 1999, SAE Paper No. 1999–01–3403.
[13] M.R. North, Disc brake squeal, a theoretical model, Technical Report 1972/5, Motor Industry Research Association, Warwickshire, England, 1972.
[14] M.R. North, Disc brake squeal, in: Braking of Road Vehicles, Automobile Division of the Institution of Mechanical Engineers, Mechanical Engineering Publications Limited, London, England, 1976, pp. 169–176.
[15] H. Ouyang, J.E. Mottershead, D.J. Brookfield, S. James, M.P. Cartmell, A methodology for the determination of dynamic instabilities in a car disc brake (special issue on Brake roughness, noise, vibration and dynamics), *International Journal of Vehicle Design* 23 (3/4) (2000) 241–262.
[16] Y. Denou, M. Nishiwaki, First order analysis of low frequency disk brake squeal, Technical Report 2001-01-3136, SAE, Warrendale, PA, 2001.